RSC Advances

This is an *Accepted Manuscript*, which has been through the Royal Society of Chemistry peer review process and has been accepted for publication.

Accepted Manuscripts are published online shortly after acceptance, before technical editing, formatting and proof reading. Using this free service, authors can make their results available to the community, in citable form, before we publish the edited article. This *Accepted Manuscript* will be replaced by the edited, formatted and paginated article as soon as this is available.

You can find more information about *Accepted Manuscripts* in the Information for Authors.

Please note that technical editing may introduce minor changes to the text and/or graphics, which may alter content. The journal's standard Terms & Conditions and the Ethical guidelines still apply. In no event shall the Royal Society of Chemistry be held responsible for any errors or omissions in this *Accepted Manuscript* or any consequences arising from the use of any information it contains.

ROYAL SOCIETY OF CHEMISTRY

www.rsc.org/advances

RSC Advances

ARTICLE

Following Ramachandran: exit vector plots (EVP) as a tool to navigate chemical space covered by 3D bifunctional scaffolds. The case of cycloalkanes

Received 00th January 20xx,
Accepted 00th January 20xx

DOI: 10.1039/x0xx00000x

www.rsc.org/

Oleksandr O. Grygorenko,[a†] Pavlo Babenko,[a] Dmitry M. Volochnyuk,[b] Oleksii Raievskyi,[c,d] Igor V. Komarov[a]

An approach to analysis and visualization of chemical space covered by disubstituted scaffolds, which is based on exit vector plots (EVP), is used for analysis of the simplest disubstituted cyclic cores – cycloalkanes, deposited in the Cambridge Structural Database (CSD). It is shown that four clearly defined regions are found in EVP of the cycloalkanes, similar to those observed in Ramachandran plots for peptides. These results can be used for directed design of more complex scaffolds, classification of conformational space for the disubstituted scaffolds, rational scaffold replacement, or SAR studies.

Introduction

The concept of chemical space, *i. e.* descriptor space covered by all the possible molecules, is widely used to analyze compound libraries in combinatorial chemistry, drug discovery and many other areas.[1–3] Due to the huge size of the chemical space, efficient strategies for its exploration and navigation,[4–9] as well as visualization[10–12] are required. Molecular scaffolds are among the tools widely used nowadays for this purpose. Initially defined by Bemis and Murcko as combinations of ring systems and linkers connecting them,[13] the scaffolds were widely used in medicinal chemistry and chemoinformatics to assess the diversity of compound libraries.[14–24]

The well-established tendency in drug discovery is related to shifting towards three-dimensional, non-flattened scaffolds in the design of the compound libraries.[25–29] A number of approaches to quantitative analysis of molecular "three-dimensionality" can be found in the literature, including the use of either very simple molecular descriptors such as fraction of sp^3 carbon atoms (Fsp^3)[25] or more sophisticated (but still convenient) parameters like principal moments of inertia,[30] plane of best fit,[31] alpha shapes,[32] ultrafast shape recognition (USR) descriptors,[33] 3D Zernike descriptors,[34] harmonic pharma chemistry coefficient (HPCC),[35] shape fingerprints,[36] torsion fingerprints (TFD),[37] radius of gyration and shadow indices.[38] Most of these descriptors consider the overall shape of the molecule and do not count for relative orientation of particular functional groups mounted onto the central molecular scaffold. However, functional groups and other fragments connected to scaffolds play the central role in the drug-target interaction. Therefore it would be useful to have simple parameters allowing quantifying relative spatial orientation of the scaffold functionalities.

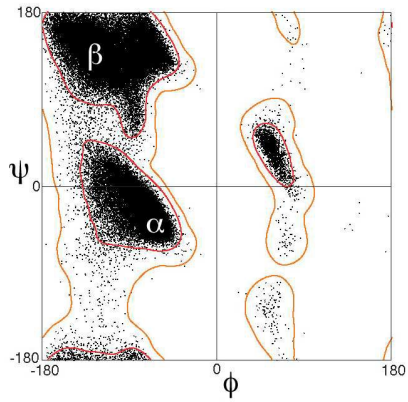

Figure 1 Ramachandran plot (reproduced from[39])

Torsion angles are the most obvious parameters which can be used to assess the relative orientation of the molecular fragments attached to the scaffold. One of the most prominent examples of using these parameters were well-known Ramachandran (φ – ψ) plots, introduced for description of peptide backbone conformation in 1960s[40] (Figure 1). These

[a] Taras Shevchenko National University of Kyiv, Volodymyrska Street 60, Kyiv 01601, Ukraine.
[b] Institute of Organic Chemistry National Academy of Sciences of Ukraine, Murmanska Street 5, Kyiv 02094, Ukraine.
[c] Institute of Molecular Biology and Genetics National Academy of Sciences of Ukraine, Zabolotnogo Street 150, Kyiv 03680, Ukraine.
[d] Life Chemicals, Life Chemicals Group, 1A Dixie Avenue, Niagara-on-the-Lake ON L0S 1J0, Canada.
[†] Correspondence and requests for materials should be addressed to O.O.G. (e-mail gregor@univ.kiev.ua).

Electronic Supplementary Information (ESI) available: the program which allows calculation of EVP geometric parameters from SDF containing 3D coordinates, together with sample files. See DOI: 10.1039/x0xx00000x

RSC Advances Accepted Manuscript

plots were convenient to use even with low calculation capacities available in those years, and they soon became a golden standard for discussing the three-dimensional structure of peptides and proteins. The use of torsion angles was extended for β- and other ω-peptides,[41] and they were also evaluated for the purposes of medicinal chemistry.[42–44]

The major drawback of torsion angles as conformational descriptors of molecular scaffolds is the fact that multiple parameters are needed in general case; moreover, their number is varied for different scaffolds. Being inspired by the idea of simple visualization of molecular geometry provided by Ramachandran plots, we turned our attention to an alternative approach based on the so-called exit vectors, introduced for CAVEAT software in 1990s.[45] Recently, we have used them for exploration of conformationally restricted diamines[46–48] and other related molecules.[49] In this approach, the functional groups mounted onto a scaffold are simulated by bound unit vectors. The variation points of the scaffold are used as the starting points of these vectors, whereas to define their directions, either the bonds to the substituents (for the carbon attachment points) or the bisectors of the corresponding valence angles (for the nitrogen attachment points, which are usually configurationally unstable) are used. In the case of bifunctional scaffolds, the relative orientation of the two exit vectors $\boldsymbol{n_1}$ and $\boldsymbol{n_2}$ can be described by four geometric parameters defined in Figure 2 for 1,2-disubstituted cyclohexane: the distance between the variation points **N1** and **N2** – r, the plane angles φ_1 (between vectors $\boldsymbol{n_1}$ and **N2N1**) and φ_2 (between $\boldsymbol{n_2}$ and **N1N2**), and the dihedral angle θ defined by vectors $\boldsymbol{n_1}$, **N1N2** and $\boldsymbol{n_2}$.[46–49] These parameters can be calculated easily from atomic coordinates and then used for the construction of Ramachandran-like plots ($r - \theta$, $\theta - \varphi_1/\varphi_2$, and $\varphi_1 - \varphi_2$) and further analysis of the library distribution over their three-dimensional geometric properties.

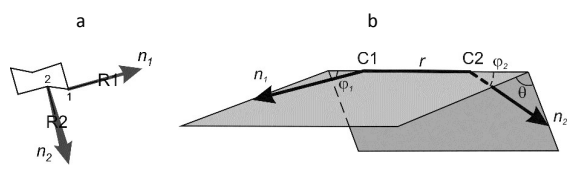

Figure 2 a) Definition of vectors $\boldsymbol{n_1}$, $\boldsymbol{n_2}$ (1,2-disubstituted cyclohexane scaffold is used as an example). b) Definition of geometric parameters r, φ_1, φ_2, and θ.

Whereas r can be used as a measure of the scaffold size, the angles φ_1, φ_2 and θ define relative spatial orientation of the exit vectors – a property which is important to all areas of chemistry where intermolecular interactions are involved. For example, in drug design, this disposition is critical for the interaction of the fragments attached to the scaffold with the biological targets. The values of φ_1, φ_2 and θ angles can be used for estimation of the scaffold shape. Thus, for linear core (1,4-disubstituted benzene), $\varphi_1 = \varphi_2 = 0°$ (θ is undefined) (Figure 3). For non-linear flat molecules (such as 1,2-disubstituted benzenes), φ_1 and φ_2 have non-zero values, whereas the absolute value of θ is close to 0° or 180°. Finally, for many disubstituted cycloalkanes (*e. g.* 1,2-disubstituted cyclohexanes) and other non-flattened scaffolds, all the three angles are far from 0° (and 180°). Analysis of such cores in terms of r, φ_1, φ_2 and θ parameters might be especially useful for molecular design in various fields, in particular, for scaffold replacement approaches or discovery of chemotypes with previously unexplored molecular geometries.

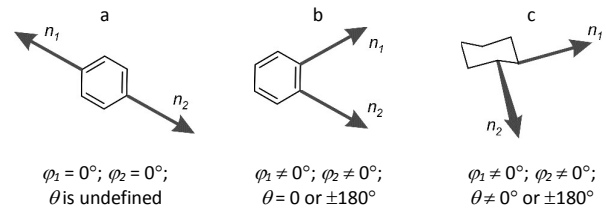

Figure 3 Parameters φ_1, φ_2, and θ as functions of the scaffold shape: a) linear; b) non-linear flat; c) non-flattened.

In this work, we report the construction and analysis of plots ("exit vector plots" (EVP) in several coordinates, $r - \theta$, $\theta - \varphi_1/\varphi_2$, and $\varphi_1 - \varphi_2$ for the simplest disubstituted cycloalkane scaffolds (cyclopropane, cyclobutane, cyclopentane, and cyclohexane), which is based on experimental data available from Cambridge Structural Database (CSD).[50] Such use of the CSD has long been proven as an efficient instrument of structural, conformational and reactivity analysis.[51] Fifty years since its establishment, the CSD has collected vast structural information (currently more than 750000 entries). Each crystal structure deposited in the CSD was obtained for different and specific purposes (mainly for structure elucidation), but with more and more structural information available, it became possible to retrieve general structural relationships by statistical CSD analyses. Here, we propose a very simple EVP-based variant of such an analysis, which can be easily visualized. In our opinion, the results of such analysis should establish the basis for further use of the method for more complex systems. We expect that some relationships in the distribution of conformations over the EVP should be elucidated, similar to α or β regions of the Ramachandran diagram used for the explanation and prediction of typical peptide secondary structure elements.

It is known that conformational space of cycloalkanes has been studied thoroughly in previous works. Strauss – Pickett torsion angles,[52] Cremer – Pople[53] and Zefirov – Palyulin – Dashevskaya (ZPD)[54] puckering parameters are the classical approaches to discuss cycloalkane conformations; some newer methods can be also mentioned such as triangular tessellation.[55] However, these approaches can hardly be applied for general analysis of the whole chemical space of the disubstituted scaffolds. In this view, their major drawbacks are similar to those of usual torsion angles discussed above. All these approaches are limited by monocyclic ring systems; multiple parameter sets are needed in general case, and the number of these parameters is varied even for different cycloalkanes.

RSC Advances Accepted Manuscript

 This journal is © The Royal Society of Chemistry 20xx

Results and discussion

Calculation of the geometric parameters

Atomic coordinates for the 1,2-disubstituted cycloalkanes were retrieved from CSD into CIF files using the substructure search. The data for each molecule were transferred into the database, and 1,2-disubstituted cycloalkane cores, as well as the variation points of exit vectors were identified using Open Babel software[56] and in-house written Ruby script. The cores with undefined positions were removed from the consideration. The corresponding atomic coordinates for 2886 disubstituted cycloalkane cores thus obtained were used to calculate the geometric parameters r, φ_1, φ_2, and θ. Since the sign of θ angle is the only parameter which is affected by the chirality of the molecule, we have considered only absolute values of the θ, keeping in mind that corresponding negative values are also possible. In other words, we took only one enantiomer from the enantiomeric pairs for the analysis. Furthermore, for the choice of the carbon atom numbers of a cycloalkane scaffold was not arbitrary, we let $\varphi_1 > \varphi_2$. The calculated values were used to construct EVP (in $r - \theta$, $\theta - \varphi_1/\varphi_2$, and $\varphi_1 - \varphi_2$ coordinates) for each of the ring systems discussed in this work and then – for the combined data set.

Discussion of EVP for particular disubstituted cycloalkane rings

Cyclopropanes and cyclobutanes. Distribution of the data points in the EVP for the small rings is trivial and corresponds to the existence of *cis*- and *trans*-isomers of 1,2-disubstituted cyclopropanes (1,2-C3), 1,2- and 1,3-disubstituted cyclobutanes (1,2- and 1,3-C4), which gives six different areas in both $r - \theta$ and $\theta - \varphi_1/\varphi_2$ plots (Figure 4; Table 1, Entries 1–6). Similar values of r, φ_1 and φ_2 are observed for all the 1,2-disubstituted cores ($r \sim 1.5$ Å, $\varphi_1/\varphi_2 \sim 60°$); nevertheless, they are easily differentiated by θ angle (*cis*-1,2-C3: $\theta \sim 0°$; *cis*-1,2-C4: $\theta \sim 25°$; *trans*-1,2-C3: $\theta \sim 140°$; *trans*-1,2-C4: $\theta \sim 100°$). Larger values of r are quite obvious for 1,3-disubstituted cyclobutanes ($r \sim 2.15$ Å). On the contrary, φ_1 and φ_2 angles are diminished, which is characteristic for more linear shape of the scaffolds, especially for the *cis*-isomer (*cis*-1,3-C4: $\varphi_1/\varphi_2 \sim 35°$; *trans*-1,3-C4: $\varphi_1 \sim 60°$, $\varphi_2 \sim 40°$). Again, both these scaffolds are strongly discriminated by θ angle, which is close to its boundary values (*cis*-1,3-C4: ~ 0°; *trans*-1,3-C4: $\theta \sim 180°$).

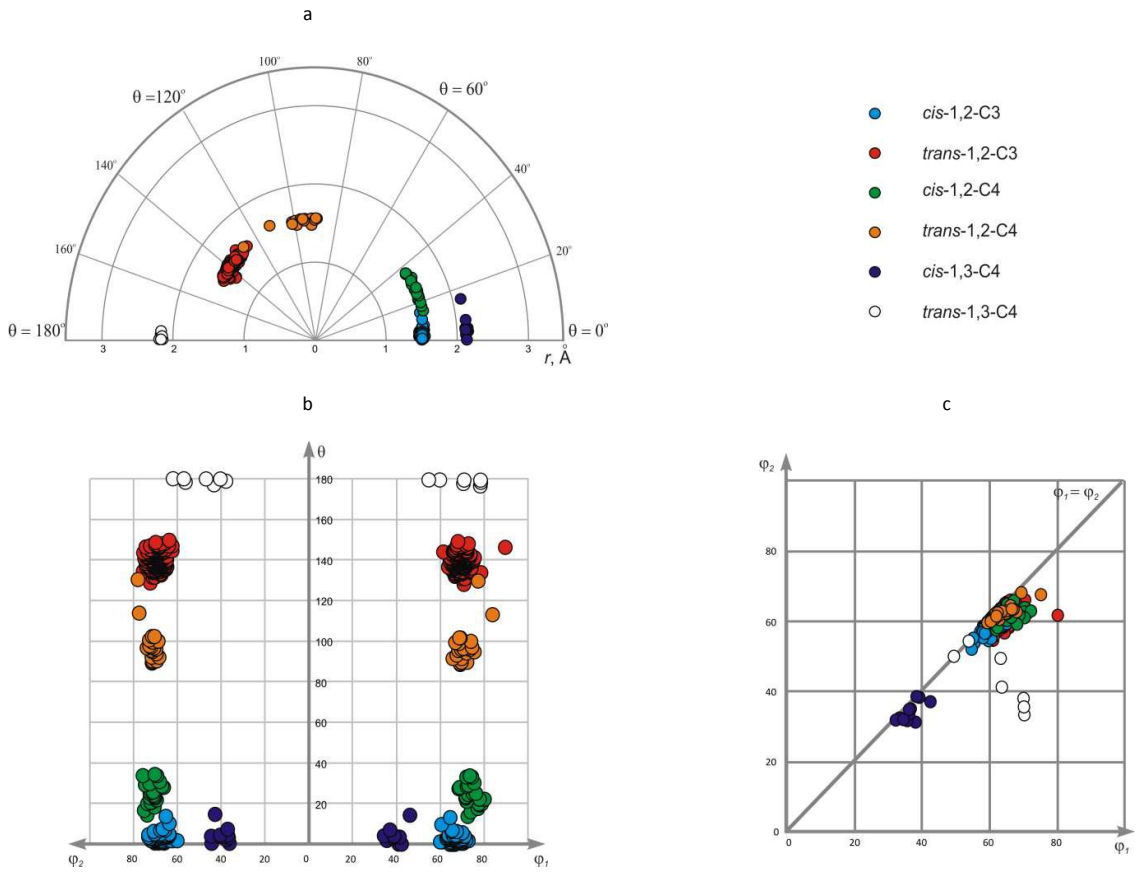

Figure 4 Disubstituted cyclopropanes and cyclobutanes shown in: a) $r - \theta$ plot (polar coordinates); b) $\theta - \varphi_1/\varphi_2$ plot; c) $\varphi_1 - \varphi_2$ plot

RSC Advances Accepted Manuscript

Table 1 Geometric parameters r, φ_1, φ_2, and θ for the disubstituted cycloalkanes (average values are given in parentheses)

No.	Ring system	No. of points	r, Å	φ_1, °	φ_2, °	θ, °
1	*cis*-1,2-C3	59	1.469–1.552 (1.513)	58.7–65.3 (59.7)	58.2–62.3 (57.6)	0–13.2 (2.7)
2	*trans*-1,2-C3	246	1.362–1.604 (1.508)	54.8–79.4 (61.5)	53.4–64.9 (59.3)	128.3–149.5 (139.9)
3	*cis*-1,2-C4	22	1.531–1.581 (1.557)	61.3–71.6 (66.4)	56.3–64.7 (60.8)	13.8–33.8 (24.4)
4	*trans*-1,2-C4	22	1.476–1.591 (1.547)	58.7–74.5 (63.5)	58.4–67.0 (61.4)	88.8–130.1 (97.7)
5	*cis*-1,3-C4	11	2.120–2.165 (2.139)	31.7–41.9 (36.0)	30.0–37.3 (33.0)	0–14.3 (4.0)
6	*trans*-1,3-C4	7	2.141–2.189 (2.167)	48.8–69.6 (62.3)	32.0–53.1 (41.9)	177.0–179.9 (179.1)
7	*cis*-1,2-C5	44	1.475–1.617 (1.548)	59.2–89.5 (68.8)	52.8–69.8 (64.6)	8.0–59.6 (39.8)
8	*trans*-1,2-C5	265	1.399–1.699 (1.539)	60.0–82.6 (68.8)	59.1–79.9 (66.8)	52.7–168.5 (96.1)
9	*cis*-1,3-C5	21	2.375–2.503 (2.425)	30.2–80.7 (56.4)	28.3–78.7 (47.0)	0–27.5 (12.9)
10	*trans*-1,3-C5	10	2.413–2.492 (2.450)	44.4–77.2 (67.2)	30.9–71.0 (46.0)	122.6–173.6 (150.9)
11	*cis*-1,2-C6	174	1.434–1.667 (1.536)	60.0–76.5 (69.3)	57.9–74.5 (67.0)	41.2–73.3 (57.4)
12	*trans*-1,2-C6	1117	1.328–1.651 (1.526)	63.0–81.0 (70.4)	55.8–75.7 (68.3)	34.4–76.8; 134.6–174.8 (62.5)
13	*cis*-1,3-C6	57	2.451–2.600 (2.522)	20.8–42.5 (36.0)	20.8–41.8 (33.9)	0–26.4 (5.0)
14	*trans*-1,3-C6	16	2.495–2.563 (2.532)	63.7–87.5 (81.7)	29.3–39.0 (35.0)	93.4–123.8 (150.9)
15	*cis*-1,4-C6	197	2.815–3.057 (2.966)	7.4–82.8 (69.8)	2.9–44.4 (24.0)	0–52.1 (3.9)
16	*trans*-1,4-C6	618	2.738–3.071 (2.960)	1.9–83.8 (30.1)	1.9–79.4 (27.9)	158.7–180.0 (177.4)

In $\varphi_1 - \varphi_2$ plot, the data points form three areas, which correspond to 1,2-disubstituted cores ($\varphi_1/\varphi_2 \sim 60°$), *cis*-1,3-C4 ($\varphi_1/\varphi_2 \sim 35°$) and *trans*-1,3-C4 ($\varphi_1 \sim 60°$, $\varphi_2 \sim 40°$) (Figure 4c). It is interesting to note that $\varphi_1 - \varphi_2$ plot is very convenient to evaluate the dissymmetry of the scaffold since only φ_1 and φ_2 parameters can distinguish the variation points. In this view, symmetric cores are located at $\varphi_1 = \varphi_2$ line, whereas dissymmetric ones are drawn away from this position. In the case of small rings, the dissymmetry is observed for *trans*-1,3-C4 scaffold, which can be explained by different (*i. e.* pseudo-axial and pseudo-equatorial) orientation of the corresponding substituents in the puckered cyclobutane fragment (Figure 5a, **1**). This is not true for two data points which refer to *trans*-1,3-cyclobutanedicarboxylic acid (**2**) and its disodium salt; in these cases, flat structure was reported by authors for the cyclobutane ring.[57,58] Although revision of these data points from late 1960s might be necessary, it is important to note that the uncommon conformations were identified simply by visual inspection – an interesting aspect of potential application of EVP.

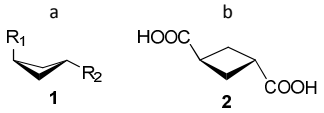

Figure 5 Conformations of *trans*-1,3-disubstituted cyclobutanes according to CSD data

Cyclopentanes. The main feature of EVP for the disubstituted cyclopentane scaffolds is related to their conformational flexibility, which gives diffuse areas formed by the data points (Figure 6; Table 1, Entries 7–10). The four possible subtypes of the templates discussed in this section (*cis*-1,2-C5, *trans*-1,2-C5, *cis*-1,3-C5, and *trans*-1,3-C5) can be more or less clearly differentiated only in $r - \theta$ plot. Since for the 1,2-disubstituted cores the values of r, φ_1 and φ_2 are defined only by C–C bond lengths and the corresponding valence angles, in the case of *cis*- and *trans*-1,2-C5 these parameters ($r \sim 1.5$ Å, $\varphi_1/\varphi_2 \sim 65°$) are similar to that for the small rings, and they do not vary significantly. The conformational flexibility is expressed mainly through θ angle values, which are kept within the following ranges: *cis*-1,2-C5 – ~0–60°; *trans*-1,2-C5 – ~60–180°. It is interesting to note that these ranges overlap for *cis*- and *trans*-isomers. For the 1,3-disubstituted cores, the value of r is slightly larger than that for the small rings ($r \sim 2.4$ Å). The values of φ_1/φ_2 angles vary considerably (~30–80°), whereas for θ, the flexibility is less pronounced than in the case of 1,2-disubstituted counterparts (*cis*-1,3-C5: ~0–30°; *trans*-1,3-C5: ~120–180°). These features do not allow discrimination of 1,2- and 1,3-disubstituted cyclopentanes in $\theta - \varphi_1/\varphi_2$ plot.

Due to the conformational flexibility of the cyclopentane ring mentioned above, it is not possible to outline some particular areas in $\varphi_1 - \varphi_2$ plot. The data points for the 1,2-disubstituted cores correspond to the symmetric nature of the scaffolds, whereas for 1,3-disubstituted ones, both symmetric (**3**, **5**, **7**, **8**) and non-symmetric (**4**, **6**) representatives are encountered (Figure 7). Again, simple visual inspection of EVP allowed for the classification of different cyclopentane conformations in this case.

Cyclohexanes. Due to the relative conformational rigidity of the cyclohexane ring, the data points in the EVP ($r - \theta$, $\theta - \varphi_1/\varphi_2$) for the disubstituted cyclohexanes form six clear and easily distinguishable clusters (with singletones also present), which might be initially addressed to existence of six possible isomeric scaffolds: *cis*-1,2-C6, *trans*-1,2-C6, *cis*-1,3-C6, *trans*-1,3-C6, *cis*-1,4-C6, and *trans*-1,4-C6 (Figure 8; Table 1, Entries 11–16). However, detailed analysis of the data revealed that this is not the case. Again, 1,2-disubstituted derivatives follow the above-discussed trends for r and φ_1/φ_2 parameters ($r \sim 1.5$ Å, $\varphi_1/\varphi_2 \sim 70°$; note slight increase of φ_1/φ_2 average values upon increasing the ring size). Nevertheless, unlike their smaller counterparts, *cis*- and *trans*-1,2-C6 scaffolds cannot be distinguished using the θ angle. All the data points for the *cis*-isomers and most – for the *trans* isomers refer to $\theta \sim 60°$, which corresponds to favorable axial-equatorial and di-equatorial

RSC Advances Accepted Manuscript

 This journal is © The Royal Society of Chemistry 20xx

RSC Advances

ARTICLE

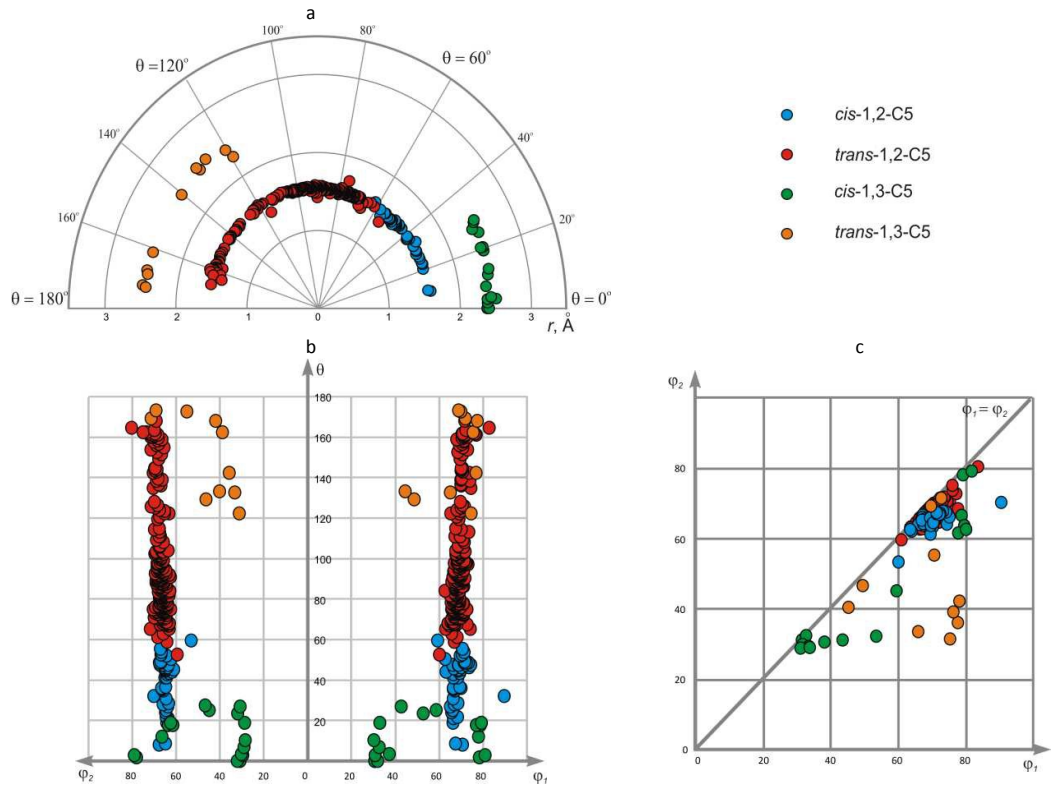

Figure 6 Disubstituted cyclopentanes shown in: a) $r - \theta$ plot (polar coordinates); b) $\theta - \varphi_1/\varphi_2$ plot; c) $\varphi_1 - \varphi_2$ plot.

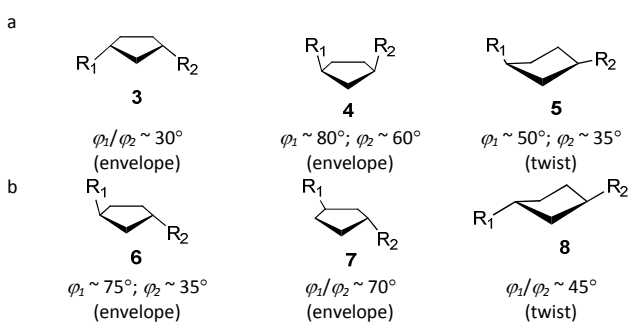

Figure 7 Conformations of a) *cis*-; b) *trans*-1,3-disubstituted cyclopentanes according to CSD data

position of the substituents, respectively, in the chair conformation. Some fraction of the compounds derived from *trans*-1,2-C6 template (44 of 1117) has $\theta \sim 160°$, which corresponds to di-axial chair **9** (Figure 9); most of these compound have very bulky substituents which destabilize di-equatorial position.

Both *cis*- and *trans*-1,3-disubstituted cyclohexanes (*cis*- and *trans*-1,3-C6) do not show significant conformational heterogeneity, although it could be related to smaller number of the data points as compared to other representatives discussed in this section. The value of r is ~ 2.5 Å, which again is slightly larger than in the case of 1,3-disubstituted derivatives of smaller rings. The values of other geometric parameters are: for *cis*-1,3-C6 – $\varphi_1/\varphi_2 \sim 35°$, $\theta \sim 0°$; for *trans*-1,3-C6 – $\varphi_1 \sim 80°$, $\varphi_2 \sim 35°$, $\theta \sim 120°$; hence these isomers have very different conformational properties. These parameters describe favorauble di-equatorial and axial-equatorial chair conformations, respectively. It is appropriate to note that the values of φ_1/φ_2 angles correlate well with axial or equatorial position of the corresponding substituent (~ 80° for axial, ~35° for equatorial). For both isomers, slightly deviating data points are observed, which correspond to the distorted conformations

RSC Advances Accepted Manuscript

RSC Advances

ARTICLE

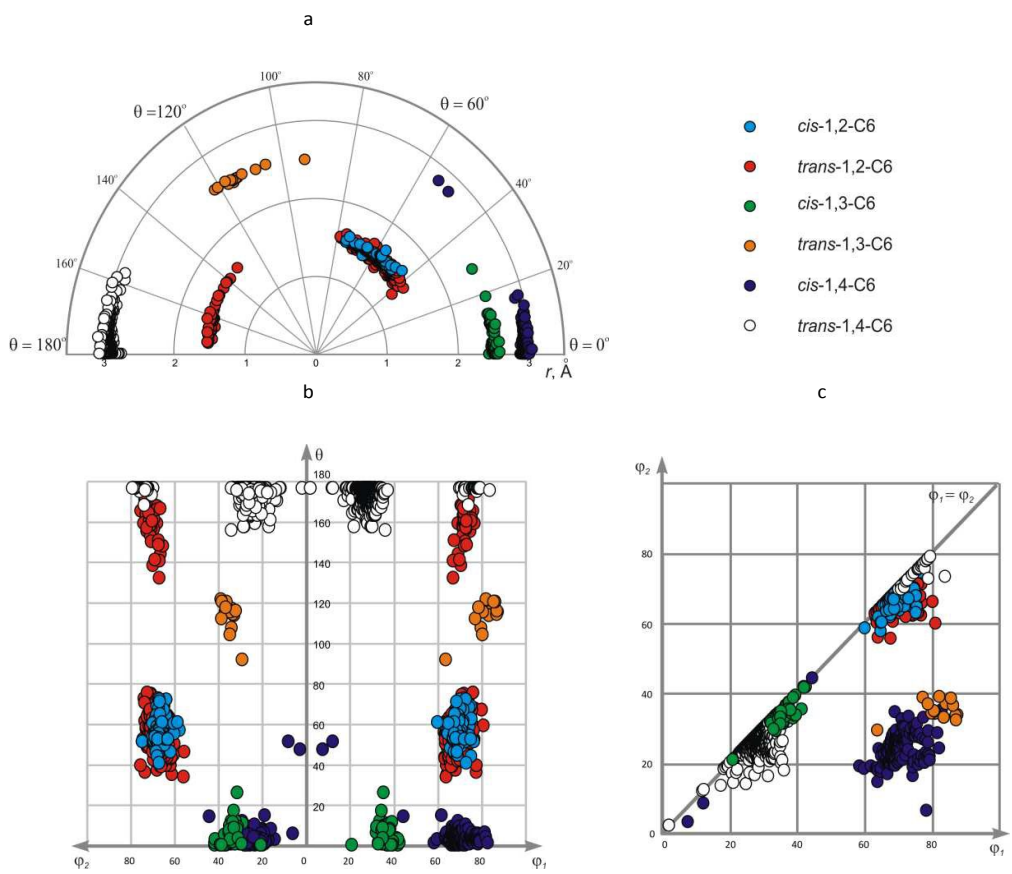

Figure 8 Disubstituted cyclohexanes shown in: a) $r - \theta$ plot (polar coordinates); b) $\theta - \varphi_1/\varphi_2$ plot; c) $\varphi_1 - \varphi_2$ plot

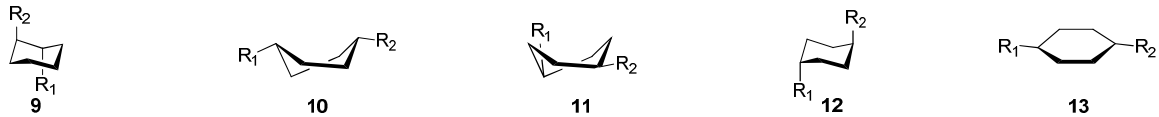

9	10	11	12	13
φ_1/φ_2 ~ 70°	φ_1/φ_2 ~ 0°	φ_1/φ_2 ~ 45°	φ_1/φ_2 ~ 75°	φ_1/φ_2 ~ 0°
θ ~ 160°	θ ~ 50°	θ ~ 15°	θ ~ 180°	θ ~ 180°
(chair, di-axial)	(twist)	("twist")	(chair, di-axial)	(nearly flat)

Figure 9 Uncommon conformations of disubstituted cyclohexanes revealed by EVP analysis of CSD data

observed in metal complexes of cyclohexane-1,3-dicarboxylates.

As in the previous cases, most of the data points for 1,4-disubstituted cyclohexanes correspond to favorauble axial-equatorial (*cis*-1,4-C6) and di-equatorial (*trans*-1,4-C6) chair conformations. The value of r is ~ 2.95 Å – for obvious reason the largest among those discussed in this work. Other parameters for the above-mentioned chair conformers are: *cis*-1,4-C6 – φ_1 ~ 70°, φ_2 ~ 25°, θ ~ 0°; *trans*-1,4-C6 – φ_1/φ_2 ~ 25°; again, the values of φ_1 / φ_2 angles correlate with axial (~ 70°) and equatorial (~ 25°) position of the corresponding substituents. The data points which do not fall into these common areas can be easily found by visual inspection of the EVP; this gives us twist conformations **10** and **11** for *cis*-1,4-

RSC Advances Accepted Manuscript

C6, di-axial chair **12** (observed for 25 compounds) and flattened ring **13** (found in a nickel complex of cyclohexane-1,4-dicarboxylate) for *trans*-1,4-C6 (Figure 9). In all these cases, it is steric strain which causes deformation of the cyclohexane ring and/or changes in position of the substituents.

According to $\varphi_1 - \varphi_2$ plot, three areas are observed; two of them (φ_1/φ_2 ~ 20–40° and ~ 60–80°, respectively) correspond to symmetric scaffolds, namely, *cis*- and *trans*-1,2-C6, *cis*-1,3-C6 and *trans*-1,4-C6; the last one (φ_1 ~ 60–90°, φ_2 ~ 20–40°) – to non-symmetric, *i. e. trans*-1,3-C6 and *cis*-1,4-C6.

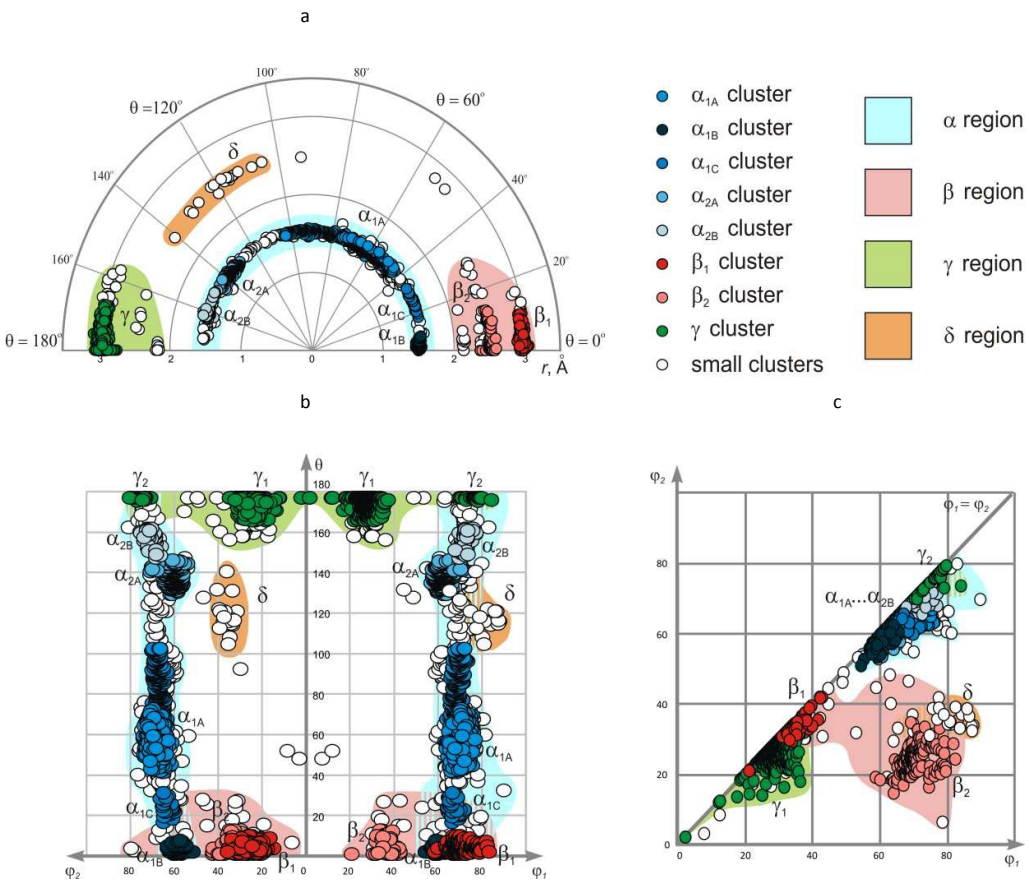

Figure 10 The combined EVP for disubstituted cycloalkanes: a) $r - \theta$ plot (polar coordinates); b) $\theta - \varphi_1/\varphi_2$ plot; c) $\varphi_1 - \varphi_2$ plot

Table 2 Results of modified Jarvis-Patrick clustering of the disubstituted cycloalkanes by geometric parameters[a]

#	Cluster	Size	*T*, Å	*r*, Å	φ_1, °	φ_2, °	θ, °
1	**α**	**1949**	**0.612**	**1.328–1.669**	**54.1–89.5**	**50.8–79.9**	**0–174.5**
2	α_{1A}	1411	0.061	1.435–1.593	63.0–76.4	60.3–73.2	41.2–103.7
3	α_{1B}	57	0.061	1.469–1.552	54.1–65.3	50.8–62.3	0–6.7
4	α_{1C}	24	0.061	1.542–1.576	64.0–71.6	59.1–65.6	16.0–30.9
5	α_{2A}	248	0.061	1.447–1.570	56.7–73.6	53.4–70.0	131.2–148.4
6	α_{2B}	48	0.061	1.439–1.601	67.5–76.8	65.1–74.6	149.5–164.4
7	**β**	**284**	**0.612**	**2.120–3.057**	**20.8–82.8**	**6.1–78.7**	**0–27.5**
8	β_1	188	0.061	2.898–3.057	58.4–82.8	14.4–35.2	0–9.2
9	β_2	58	0.061	2.377–2.600	20.8–42.5	20.8–41.8	0–12.0
10	**γ**	**630**	**0.612**	**2.141–3.071**	**1.9–83.8**	**1.9–79.4**	**160.0–180.0**
11	γ	596	0.061	2.738–3.071	1.9–83.8	1.9–79.4	168.4–180.0
12	**δ**	**18**	**0.612**	**2.413–2.563**	**65.0–87.5**	**30.9–39.0**	**106.0–142.7**

[a]Cartesian coordinates (x, y, z, t) in four-dimensional space, where $x = r\sin\varphi_1\sin\varphi_2\sin\theta$; $y = r\sin\varphi_1\cos\varphi_2\sin\theta$; $z = r\cos\varphi_1\sin\theta$; $t = r\cos\theta$. Maximum dissimilarity between the data points d_{max} = 6.122 Å. The threshold parameter value T = 1% or 10% of d_{max} (0.061 Å and 0.612 Å, respectively). The minimum ratio of numbers of common neighbors for the two compounds R_{min} = 0.5.

RSC Advances Accepted Manuscript

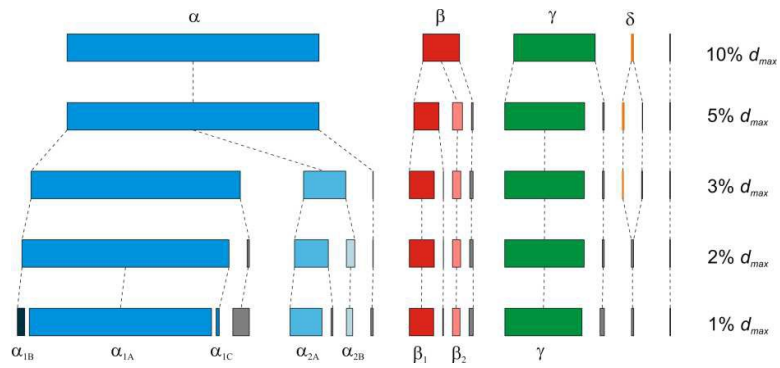

Figure 11 Clustering of the disubstituted cycloalkanes as a function of the threshold parameter *T* (varied from 10% to 1% of d_{max}). R_{min} = 0.5, d_{max} = 6.122 Å. Small clusters with no more than 10 compounds are shown in grey.

Combined EVP for the disubstituted cycloalkanes

In the previous sections, distribution of the data points in EVP was discussed considering the particular conformations of the corresponding cycloalkane scaffolds. Nevertheless, the main advantage of EVP is a possibility to give general characterization of conformational properties for large sets of diverse scaffolds. For more comprehensive analysis of the combined EVP for the disubstituted cycloalkanes, we have performed clustering of the data using a modification of the standard Jarvis-Patrick algorithm, which utilized variable-length nearest-neighbor lists.[59,60] The clustering of the data was performed using Jarp tool of JChem package.[61] To unify the coordinates for the metric distance function necessary for the clustering, the hyperspherical coordinate system defined by r, φ_1, φ_2, and θ was transformed to the Cartesian (x, y, z, t) (see our previous work[46] for more details). Standard Euclidean distance d in this four-dimensional space was used to establish the dissimilarity of the data points. The maximum dissimilarity between the data points was found to be d_{max} = 6.122 Å. The threshold parameter T of the modified Jarvis-Patrick clustering was set to 10% of this value (0.612 Å), and the ratio of numbers of common neighbors for the two compounds R_{min} – to 0.5. In addition, the T parameter was varied to be 5%, 3%, 2% and 1% of d_{max} in order to evaluate the stability of the clusters obtained.

The results of the clustering are summarized in Table 2 and used for the coloring of the data points in Figure 10. At the clustering parameter values given above, the data points split into seven clusters, three of which contain no more than two representatives. Four main clusters included 1949, 284, 630 and 18 compounds; we designated them as α, β, γ, and δ regions of the EVP, respectively. The cluster α is formed by all the 1,2-disubstituted cycloalkanes, and hence parameters r, φ_1 and φ_2 are not varied significantly within it: r ~ 1.5 Å; φ_1 / φ_2 ~ 65°. On the contrary, for the θ angle, nearly all possible values within 0–180° range are observed. These results show that for 1,2-disubstituted cores, nearly all the possible mutual orientations of the substituents can be in principle achieved using monocyclic compounds; in this case, more complex analogs can be designed only to stabilize particular values of the θ angle.

Under more strict clustering conditions (*i. e.* by decreasing T to 3% of d_{max}), the α cluster splits into two parts (Figure 11) (some small clusters with no more than 10 members are also formed). Further decrease of T to 1% of d_{max} leads to additional cluster decomposition, so that five clusters with more than 10 compounds, as well as over 100 smaller ones are obtained (Table 2, Figure 11). The largest of them, α_{1A}, is formed by 1411 data points, which have θ value ~40–100° and correspond to the following scaffolds: *cis*-1,2-C5, *cis*-1,2-C6, *trans*-1,2-C5, and *trans*-1,2-C6. Although the other clusters have smaller size, this might be related to lower occurrence of the corresponding cores in CSD, not to their lesser importance. Indeed, the clusters α_{1B} (θ ~ 0°), α_{1C} (θ ~ 20°), and α_{2A} (θ ~ 140°) correspond mainly to the cyclopropane and cyclobutane derivatives: *cis*-1,2-C3, *cis*-1,2-C4, and *trans*-1,2-C3, respectively, whereas α_{2B} (θ ~ 160°) is related to *trans*-1,2-C5 and *trans*-1,2-C6 cores with di-(pseudo)axial orientation of the substituents.

The β cluster is formed by *cis*-1,3-disubstituted scaffolds, as well as *cis*-1,4-C6. It shows less stability and splits into two parts β_1 and β_2 (and several small groups of data points) already at T = 5% of d_{max}. On the contrary, these subunits demonstrate significant stability towards the change of the clustering parameters up to T = 1% of d_{max}. The β_1 (r ~ 3.0 Å, φ_1 ~ 70°, φ_2 ~ 25°, θ ~ 0°) and β_2 (r ~ 2.5 Å, φ_1 / φ_2 ~ 35°, θ ~ 0°) clusters are formed by the data points derived almost exclusively from *cis*-1,4-C6 and *cis*-1,3-C6 scaffolds, respectively. Other *cis*-1,3-disubstituted scaffolds give only small clusters at this threshold parameter value.

Unlike its α and β counterparts, the γ cluster, which is formed by *trans*-1,4-C6 derivatives, demonstrates considerable stability towards the change of the clustering parameters: only a few small groups of data points split out upon decreasing T from 10% to 1% of d_{max}. Despite this stability, visual inspection of EVP shows that the compounds are distributed unevenly within the resulting γ cluster. Namely, two groups of the data points are observed which differ by φ_1 / φ_2 values. The larger one (γ_1, 573 rings) with φ_1 / φ_2 ~ 30° corresponds to the di-equatorial orientation of the substituents in the chair conformation of the cyclohexane, whereas the smaller one (γ_2, 20 rings, φ_1 / φ_2 ~ 75°) – to the di-axial. This difference is clearly seen only in θ–φ_1/φ_2 and φ_1 – φ_2 plots, since r and θ values do not show

RSC Advances Accepted Manuscript

This journal is © The Royal Society of Chemistry 20xx

significant deviation from the average values (r ~ 3.0 Å; θ ~ 180°).

The δ cluster, which is formed only by 18 data points (at T = 10% of d_{max}), does not demonstrate sufficient stability towards more rigorous clustering conditions. Nevertheless, one of the possible reasons behind this could be the fact that it includes the derivatives of *trans*-1,3-C6 and (partially) *trans*-1,3-C5 cores, which are not numerous in CSD. That is why, in our opinion, the δ region of EVP, which corresponds to r ~ 2.5 Å, φ_1 ~ 80°, φ_2 ~ 35°, θ ~ 120°, is worth outlining.

Analysis of the β, γ, and δ regions of EVP shows that unlike the α area, they do not cover all the values of θ angle. In particular, the θ ~ 40–100° range, which is represented well in the α region of the map, is virtually empty for larger r values characteristic for the β, γ, and δ areas. Therefore, design of the scaffolds with $r > 2$ Å can be aimed at filling such empty regions.

In the φ_1 – φ_2 plot, the clusters discussed above are not observed separately. In particular, all subunits of the α region overlap with each other, as well as the γ_2 group and many small clusters with φ_1 / φ_2 ~ 60–80°. Analogously, β_1 and γ_1 clusters (φ_1 / φ_2 ~20–40°) are also overlapped. All these data sets correspond to the symmetric scaffolds; in the case of non-symmetric ones, the two areas, namely, β_2 and δ, can in principle be distinquished (φ_1 ~ 60–85°, φ_2 ~ 20–40°). It is worth noting that such non-symmetric disubstituted cycloalkane scaffolds are not numerous in CSD.

Conclusions and perspectives

Exit vector plot (EVP) analysis can be a useful tool for study and visualization of conformational properties of three-dimensional scaffolds. It is based on very simple geometrical model and can rely on either theoretical or experimental data on atomic coordinates of the molecules. EVP analysis of the CSD data for disubstituted cycloalkanes revealed four clearly defined and isolated regions in the diagrams (α, β, γ, and δ areas), unlike in the case of bicyclic conformationally restricted diamines studied in our previous work,[46]. The EVP analysis can be used in various areas where spatial arrangement of molecular fragments is important, especially those where intermolecular interactions are involved, including medicinal, supramolecular and coordination chemistry, asymmetric synthesis and conformational analysis. Possible directions of EVP use are listed below:

- EVP analysis gives an opportunity for easy identification of unusual conformers with abnormal geometric parameters. Figure 9 of this work illustrates some examples.
- EVP analysis of disubstituted cycloalkanes (as well as other simple ring systems) can be used as a guide for the design of more complex (*e. g.* bicyclic) scaffolds. In particular, we have shown that 1,2-disubstituted cores (α area of EVP) evenly cover the theoretically accessible conformational space, hence their analogues can be used only to stabilize particular conformations. For other disubstituted cycloalkanes with r > 2 Å, many empty regions are found, and the respective bi- or polycyclic analogues might fill these gaps.
- EVP can be used for classification of conformational space covered by disubstituted scaffolds, regardless of their composition. This could be especially useful for the analysis of large data sets related to biological activity (e. g. compound libraries in medicinal chemistry). In our opinion, the α, β, γ, and δ regions defined in this work might be extended by further data, but their principal location in the diagram should not change significantly. In particular, the data points for the *cis*- and *trans*-1,2-disubstituted cycloheptanes available from CSD fit well into the α area, analogously to the corresponding *cis*- and *trans*-1,2-C6 derivatives (Figure 12). For the *trans*-1,4-C7 scaffold, two data points are available: one can be considered as analogous to γ area, another does not fall into any of the regions introduced. Possibly, it might fall into extended δ area which included larger r values.
- Rational scaffold replacement is possible with the guide of EVP data. In particular, we have recently shown that various isomers of 1,6-disubstituted spiro[3.3]heptanes can be potential surrogates of either *cis*-1,4-C6 or *trans*-1,3-C6 scaffolds.[48] Using the terms introduced in this work, the corresponding isomers fall into β and δ areas of the EVP.
- EVP data can assist in building structure-property relationships, if spatial arrangement of the functional groups is the factor which affects significantly the particular property. This aspect is important first of all to medicinal chemistry, but it can be also used for prediction of *e. g.* physico-chemical parameters. Recently, we have shown that Euclidean distance d in (x, y, z, t) space (easily obtained from r, φ_1, φ_2, θ coordinates) shows good correlation with biological activity for nicotine acetylcholine receptor ligands.[46] Notably, for the fluoroquinolone antibiotics, where arrangement of the substituent around the diamine scaffold does not affect biological activity significantly since it is not involved into the mechanism of action, no such correlation was observed. In this work, we give one more example derived from cycloalkane scaffolds discussed in this work, namely, chemokine receptor CKCR3 antagonists **14** (Figure 13) taken from the Sanofi patent.[62] The parameters r, φ_1, φ_2, θ for these compounds were evaluated using average values for the corresponding scaffolds given in Table 1. A correlation with r^2 = 0.515 was found between relative biological activity and parameter d for these series, which shows that relative orientation of the functional groups attached to the cycloalkane scaffold plays important role in interaction of **14** with their biological target. For this particular case, the optimal cycloalkane scaffolds are located near γ region of EVP.[63]

To help the readers in using exit vector plots (EVP) for their own analysis of scaffolds, we have provided a program which calculates all the necessary geometric parameters (r, φ_1, φ_2, θ) from SDF containing 3D coordinates (see ESI for more details).

RSC Advances Accepted Manuscript

RSC Advances

ARTICLE

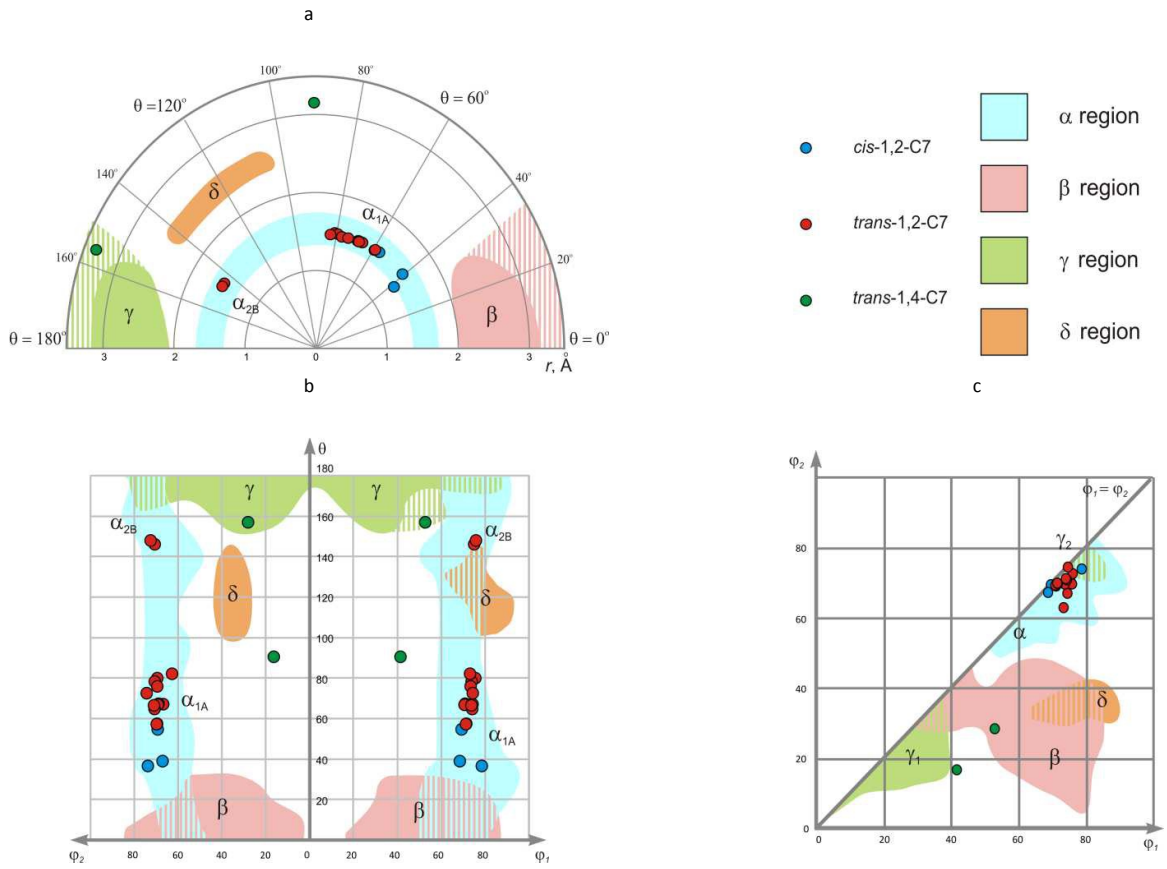

Figure 12 The EVP for disubstituted cycloheptanes: a) $r - \theta$ plot (polar coordinates); b) $\theta - \varphi_1/\varphi_2$ plot; c) $\varphi_1 - \varphi_2$ plot

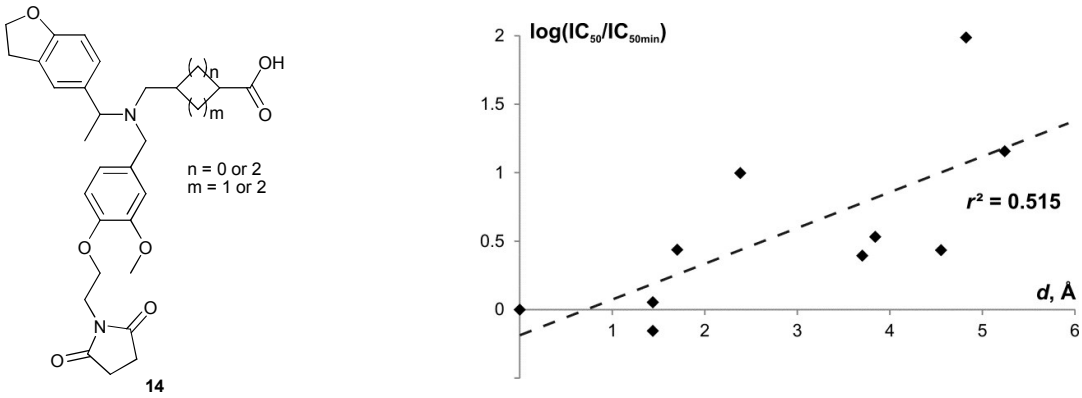

Figure 13 Correlation between the relative biological effect of the chemokine receptor CXCR3 antagonists **14** ($\log(IC_{50}/IC_{50min})$) and the Euclidean distance of the corresponding cycloalkane scaffolds from the scaffold of the most active compound (d)[64]

RSC Advances Accepted Manuscript

RSC Advances

ARTICLE

Notes and references

1 P. Kirkpartick and C. Ellis, *Nature* 2004, **432**, 823.
2 C. M. Dobson, *Nature,* 2004, **432**, 824.
3 J.-L. Reymond, R. van Deursen, L. C. Blum and L. Ruddigkeit, *Med. Chem. Commun.* 2010, **1**, 30.
4 D. J. Triggle, *Biochem. Pharmacol.* 2009, **78**, 217.
5 L. Eberhardt, K. Kumar and H. Waldmann, *Curr. Drug Targets* 2011, **12**, 1531.
6 J. L. Medina-Franco, Chemoinformatic characterization of the chemical space and molecular diversity of compound libraries. In: Diversity-oriented synthesis: basics and applications in organic synthesis, drug discovery, and chemical biology (ed A. Trabocchi), John Wiley & Sons, Inc., Hoboken, NJ, USA (2013).
7 J. L. Medina-Franco, *Drug. Dev. Res*. 2012, **73**, 430.
8 Y.-S. Wong, *Methods Mol. Biol*. 2012, **800**, 11.
9 M. Dow, M. Fisher, T. James, F. Marchetti and A. Nelson, *Org. Biomol. Chem*. 2012, **10**, 17.
10 M. A. Koch, A. Schuffenhauer, M. Scheck, S. Wetzel, M. Casaulta, A. Odermatt, P. Ertl and H. Waldmann, *Proc Natl Acad Sci USA* 2005, **102**, 17272.
11 J. L. Medina-Franco, K. Martinez-Mayorga, M. A. Giulianotti, R. A. Houghten and C. Pinilla, *Curr. Comp. Aid. Drug Des*. 2008, **4**, 322.
12 R. van Deursen, L. C. Blum and J.-L. Reymond, *J. Comp. Aid. Mol. Des.* 2011, **25**, 649.
13 G. W. Bemis and M. A. Murcko, *J. Med. Chem*. 1996, **39**, 2887.
14 S. R. Langdon, N. Brown and J. Blagg, *J. Chem. Inf. Model*. 2011, **51**, 2174.
15 M. Krier, G. Bret and D. Rognan, *J Chem. Inf. Model*. 2006, **46**, 512.
16 P. Ertl, A. Schuffenhauer and S. Renner, *Methods Mol. Biol*. 2011, **672**, 245.
17 R. D. Taylor, M. MacCoss and A. D. Lawson, *J. Med. Chem*. 2014, **57**, 5845.
18 V. Khanna and S. Ranganathan, *J. Cheminform*. 2011, **3**, 30.
19 D. K. Agrafiotis and J. J. Wiener, *J. Med. Chem*. 2010, **53**, 5002.
20 H. Zhao and I. Akritopoulou-Zanze, *Expert Opin. Drug Discov*. 2010, **5**, 123.
21 S. Wetzel, K Klein, S Renner, D Rauh, T. I. Oprea, P. Mutzel and H. Waldmann, *Nat. Chem. Biol*. 2009, **5**, 581.
22 S. N. Pollock, E. A. Coutsias, M. J. Wester and T. I. Oprea, *J. Chem. Inf. Model*. 2008, **48**, 1304.
23 M. J. Wester, S. N. Pollock, E. A. Coutsias, T. K. Allu, S. Muresan and T. I. Oprea, *J. Chem. Inf. Model*. 2008, **48**, 1311.
24 C. M. Marson, *Chem. Soc. Rev*. 2011, **40**, 5514.
25 F. Lovering, J. Bikker and C. Humblet, *J. Med. Chem*. 2009, **52**, 6752.
26 K. Kingwell, *Nature Rev. Drug Discovery* 2009, **8**, 931.
27 A. Nicholls, G. B. McGaughey, R. P. Sheridan, A. C. Good, G. Warren, M. Mathieu, S. W. Muchmore, S. P. Brown, J. A. Grant, J. A. Haigh, N. Nevins, A. N. Jain and B. Kelley, *J. Med. Chem.* 2010, **53**, 3862.
28 M. Aldeghi, S. Malhotra, D. L. Selwood and A. W. Chan, *Chem. Biol. Drug Des*. 2014, **83**, 450.
29 F. Lovering, *Med. Chem. Commun*. 2013, **4**, 515.
30 W. H. Sauer and M. K. Schwarz, *J. Chem. Inf. Comput. Sci*. 2003, **43**, 987.
31 N. C. Firth, N. Brown and J. Blagg, *J. Chem. Inf. Model*. 2012, **52**, 2516.
32 J. A. Wilson, A. Bender, T. Kaya and P. A. Clemons, *J. Chem. Inf. Model*. 2009, **49**, 2231.
33 P. J. Ballester and W. G. Richards, *J. Comput. Chem.* 2007, **28**, 1711.
34 V. Venkatraman, P. R. Chakravarthy and D. Kihara, *J. Cheminf*. 2009, **1**, 19.
35 A. S. Karaboga, F. Petronin, G. Marchetti, M. Souchet and B. Maigret, *J. Mol. Graph. Model*. 2013, **41**, 20.
36 C. M. Richardson, M. J. Lipkin and D. W. Sheppard, *Bioorg. Med. Chem. Lett.* 2015, **25**, 2089.
37 T. Schulz-Gasch, C. Schärfer, W. Guba and M. Rarey, *J. Chem. Inf. Model.* 2012, **52**, 1499.
38 D. C. Kombo, K. Tallapragada, R. Jain, J. Chewning, A. A. Mazurov, J. D. Speake, J. D. Hauser and S. Toler, *J. Chem. Inf. Model*. 2013, **53**, 327.
39 S. C. Lovell, I. W. Davis, W. B. Arendall, P. I. W. De Bakker, J. M. Word and M. G. Prisant, *Proteins Struct. Funct. Genet*. 2003, **50**, 437.
40 G. N. Ramachandran, C. Ramakrishnan and V. Sasisekharan, *J. Mol. Biol*. 1963, **7**, 95.
41 A. Banerjee and P. Balaram, *Curr. Sci*. 1997, **73**, 1067.
42 S. J. Cottrell, T. S. G. Olsson, R. Taylor, J. C. Cole and J. W. Liebeschuetz, *J. Chem. Inf. Model*. 2012, **52**, 956.
43 R. Taylor, J. Cole, O. Korb and P. McCabe, *J. Chem. Inf. Model.* 2014, **54**, 2500.
44 C. Schärfer, T. Schulz-Gasch, H.-C. Ehrlich, W. Guba, M. Rarey and M. Stahl, *J. Med. Chem*. 2013, **56**, 2016.
45 G. Lauri and P. A. Bartlett, *J. Comp. Aided Mol. Design* 1994, **8**, 51.
46 O. O. Grygorenko, R. Prytulyak, D. M. Volochnyuk, V. Kudrya, O. V. Khavryuchenko and I. V. Komarov, *Mol. Divers*. 2012, **16**, 477.
47 D. S. Radchenko, S. O. Pavlenko, O. O. Grygorenko, D. M. Volochnyuk, S. V. Shishkina, O. V. Shishkin and I. V. Komarov, *J. Org. Chem*. 2010, **75**, 5941.
48 A. V. Chernykh, D. S. Radchenko, O. O. Grygorenko, C. G. Daniliuc, D. M. Volochnyuk and I. V. Komarov, *J. Org. Chem*. 2015, **80**, 3974.
49 V. S. Yarmolchuk, I. L. Mukan, O. O. Grygorenko, A. A. Tolmachev, S. V. Shishkina, O. V. Shishkin and I. V. Komarov, *J. Org. Chem*. 2011, **76**, 7010.
50 F. H. Allen, *Acta Cryst*. B 2002, **58**, 380.
51 F. H. Allen, O. Kennard and R. Taylor, *Acc. Chem. Res*. 1983, **16**, 146.
52 H. L. Strauss and H. M. Pickett, *J. Chem. Phys.* 1971, **55**, 324.
53 D. Cremer and J. A. Pople. *J. Am. Chem. Soc.* 1975, **97**, 1354.
54 N. S. Zefirov, V. A. Palyulin, E. E. Dashevskaya, *J. Phys. Org. Chem.* 1990, **3**, 147.
55 P. Khalili, C. B. Barnett and K. J. Naidoo, J. Chem. Phys. 2013, **138**, 184110.
56 N. M. O'Boyle, M. Banck, C. A. James, C. Morley, T. Vandermeersch and G. R. Hutchison, *J. Cheminf*. 2011, **4**, 33.

RSC Advances Accepted Manuscript

57 T. N. Margulis and M. S. Fisher, *J. Am. Chem. Soc*. 1967, **89**, 223.
58 E. Adman and T. N. Margulis, *J. Am. Chem. Soc*. 1968, **90**, 4517.
59 R. A. Jarvis and E. A. Patrick, *IEEE Trans. Comput*. 1973, **C22**, 1025.
60 J. M. Barnard and G. M. Downs, *J. Chem. Inf. Comput. Sci*. 1997, **37**, 141.
61 JChem, version 15.3.16.0, build date: 2015-03-16. ChemAxon, Budapest, Hungary. http://www.chemaxon.com (2015).
62 I. Bata, P. Buzder-Lantos, A. Vasas, B. V. Bartané, G. Ferenczy, Z. Tömösközi, G. Szeleczky and S. Batori. Eur. Pat. 2601950, 2013.
63 To be more precise, it is (–)-γ region, where (–) is for the sign of θ value which should be taken into account for biological activity since it describes chirality of the molecule.
64 The relative biological effect is measured as lg(IC_{50}/IC_{50min}), where IC_{50min} is the IC_{50} value for the most active compound). The Euclidean distance d is determined in the Cartesian space (x, y, z, t); $x = r\sin\varphi_1\sin\varphi_2\sin\theta$; $y = r\sin\varphi_1\cos\varphi_2\sin\theta$; $z = r\cos\varphi_1\sin\theta$; $t = r\cos\theta$. The sign of θ angle was taken into account for different enantiomers. For the mixtures of stereoisomers, average values of d were used.

RSC Advances Accepted Manuscript

This journal is © The Royal Society of Chemistry 20xx

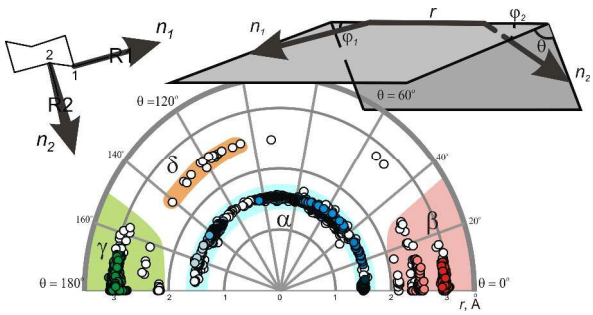

An approach to analysis and visualization of chemical space covered by disubstituted scaffolds, which is based on exit vector plots (EVP), is used for analysis of cycloalkane scaffolds. Four clearly defined regions (α, β, γ, and δ) are found in EVP of the cycloalkanes.

RSC Advances Accepted Manuscript